

Supporting Information

Probing the Binding Mode and Unbinding Mechanism of LSD1 Inhibitors by Combined Computational Methods

Xudong Sun, Lina Ding,^{*} Hong-Min Liu^{*}

Collaborative Innovation Center of New Drug Research and Safety Evaluation, Henan Province, Key Laboratory of
Technology of Drug Preparation (Zhengzhou University), Ministry of Education of China, Key Laboratory of Henan
Province for Drug Quality and Evaluation, School of Pharmaceutical Sciences, Zhengzhou University, Zhengzhou
450001, PR China

S1. Docking Simulation with Software GOLD.

Preparation Process

The docking study was also performed through GOLD 5.3 package. Prior to docking, the protein was prepared by deleting water molecules and adding hydrogen atoms. The docking site was defined as spheres with a 10 Å radius around cofactor FAD. And the accuracy and suitability of GOLD to the present system was also confirmed by the reproducing ability of FAD conformation with RMSD 1.30 Å. Among Genetic algorithm (GA) parameters, population size was increased to 1000, the operations number was set to 100000, and all the other parameters were remained default. GoldScore was used to rank the docking poses, and the top ten poses for each compound were retained for analysis.

Analysis about the Docking Results.

The docking results of the ten compounds were listed in **Table S2**. The indicated two types of conformations also presented obvious advantages among the top scored poses, which agrees with the result by MOE (**Table S1**) and further confirmed the reasonability of the proposed binding modes.

Table S1. The docking results of MOE. The number of the two types of conformations among the top-10 docking results for the ten compounds. Note: analogues were generally considered to bind to receptor in similar pose.

Compound	Type A	Type B	The Highest scored pose
1	3	5	Type B (S= -12.1)
2	4	3	Type B (S= -10.4)
3	5	2	Type B (S= -10.3)
4	4	2	Type B (S= -11.3)
5	4	4	Type B (S= -11.2)
6	1	3	Type B (S= -10.2)
7	5	2	Type B (S= -10.5)
8	5	1	Type B (S= -11.1)
9	3	3	Type B (S= -10.9)
10	4	1	Type A (S= -10.1)

Table S2. The docking results of GOLD. The number of the two types among the top-10 docking results for the ten compounds. (— represent the highest scored pose not similar to any of the two speculated binding types. For compound5, the highest scored pose similar to the proposed two conformation types was type B which is the third highest solution of the entire docking results. For compound8, the highest scored pose similar to the proposed two conformation types was type B which is the second highest solution of the entire docking results.).

Compound	Type A	Type B	The Highest Scored Pose
1	1	5	Type B (S= 93.62)
2	4	2	Type B (S= 90.27)
3	5	3	Type B (S= 85.11)
4	0	7	Type B (S= 94.43)
5	3	3	—
6	5	2	Type A (S= 84.52)
7	4	4	Type B (S= 89.24)
8	1	4	—
9	3	3	Type B (S= 90.01)
10	6	2	Type A (S= 85.49)

S2. The Detailed Interactions of Compound2 with LSD1 after Docking Simulation.

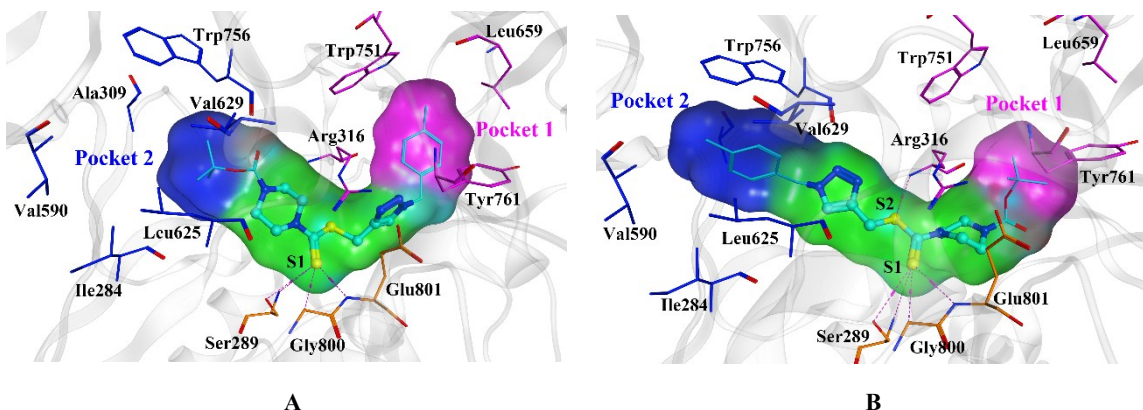


Figure S1. The speculated possible binding Type A (A) and Type B (B) forming the favorable interactions with LSD1. Compound2 was shown in cyan, and the scaffold was displayed in ball and stick model. The surface and residues of hydrophobic Pocket 1 was depicted in purple, and the hydrophobic Pocket 2 was shown in blue.

The most potent compound 2 was used to explain the detailed interactions of the series of compounds with LSD1. As shown in **Figure S1A**, compound 2 bound to the FAD-binding pocket adopting conformation Type A. The sulfur atom S1 on the double bond formed H-bonds net with residues Ser289, Gly800 and Glu801. The t-butoxy located in a hydrophobic Pocket 2 consisting of residues Ile284, Ala309, Val590, Leu625, Val629 and Trp756, while the phenyl occupied the hydrophobic Pocket 1 consisting of residues Leu659, Trp751, Tyr761 and the sidechain of residue Arg316. Furthermore, the triazole ring toward to the sidechain of residue Arg316 which is derived from the electrical match and the tendency to form H-bond interaction considering their closer distance. As for conformation Type B (**Figure S1B**), the triazole ring also had the potential to form H-bond with the sidechain of residue Arg316 considering the docking results and the flexibility of Arg316. And the sulfur

atom S1 formed the same H-bonds net as Type A with residues Ser289, Gly800 and Glu801. In addition, extensive hydrophobic and VDW interactions were also observed. The phenyl formed extensive hydrophobic interactions with the residues of hydrophobic Pocket 2, while the t-butoxy was surrounded by hydrophobic residues Leu659, Trp751, Tyr761 and the sidechain of residue Arg316 (Pocket 1).

S3. The Equilibrium Time and RMSD Value for the 20 Systems

Table S3. The equilibrium time and RMSD value of the backbone of LSD1 during MD simulation course for the 20 systems.

Compound	Equilibrium Time (ns)		RMSD (Å)	
	Type A	Type B	Type A	Type B
1	7	13	1.8	1.5
2	8	10	1.7	1.5
3	11	15	1.8	1.4
4	9	12	2	1.8
5	10	11	1.7	1.5
6	12	10	1.6	1.6
7	12	11	2	1.6
8	10	12	1.5	1.5
9	12	10	1.4	1.6
10	5	9	1.9	1.5

Table S4. The equilibrium time and RMSD value of the ten ligands for both types during MD simulation course.

Compound	Equilibrium Time (ns)		RMSD (Å)	
	Type A	Type B	Type A	Type B
1	12	19	2	0.8
2	8	12	1.5	1.2
3	10	16	1.7	1.6
4	7	18	1.5	0.8
5	10	18	1.1	0.8
6	16	14	1.3	1.2
7	16	13	2	1.3
8	12	11	0.9	0.8
9	19	6	1.6	1.5

S4. Analysis about the Interactions after MD Simulation.

The detailed binding modes for both two binding conformation types after MD simulation were elucidated by compound 2 undergoing 110ns MD simulation. As depicted in **Figure S2A** and **B**, a stable H-bond formed by N1 atom of triazole of compound 2 (N2 in type A, N1 in type B) with Arg316 presented in both binding poses as we guessed due to the strong flexibility of the sidechain of Arg316. Meanwhile, the similar but just reversed hydrophobic interactions were also formed by the two binding poses with LSD1. Hydrophobic Pocket 2 consisting of residues Ile284, Ala309, Val590, Leu625, Val629 and Trp756 was occupied by t-butoxy in Type A and phenyl in Type B, while hydrophobic Pocket 1 consisting of residues Leu659, Trp751, Tyr761 and Arg316 was occupied by phenyl in Type A and t-butoxy in Type B. Apart from the mentioned similarity, however, two relatively stable H-bonds mediated by waters were observed in Type B but not in Type A which strengthen the presence of Type B. And the H-bonds net observed in the initial conformations between the sulfur atom S1 and LSD1 all disappeared except the H-bond with residue Ser289 in Type B. Although, the potency of the H-bonds formed by S1 atom with Ser289 was a little weak.

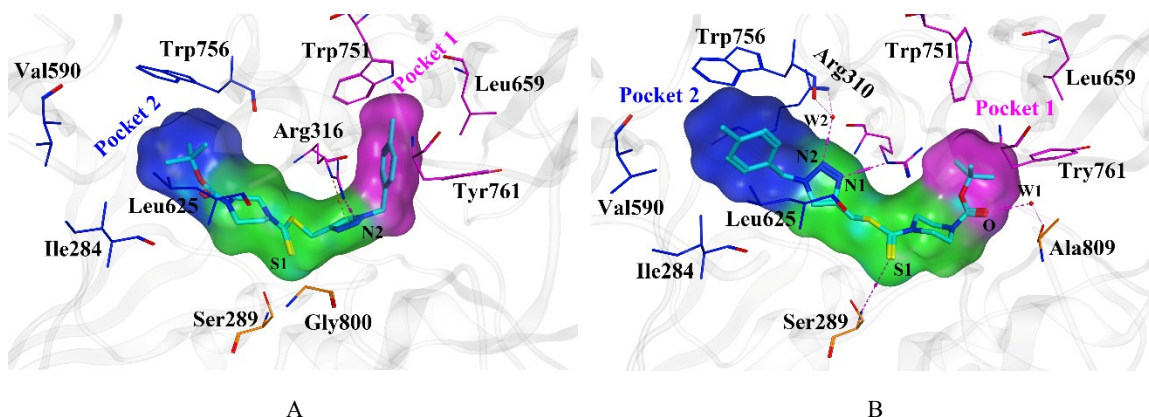


Figure S2. The detailed binding modes of compound2 in Type A (A) and B (B) after MD simulations. Compound2 was shown in cyan. The surface and residues of hydrophobic Pocket 1 was depicted in purple, and the hydrophobic Pocket 2 was shown in blue.

S5. The Influence of the Activity Span to the Correlation between $\langle W \rangle$ and ΔG_{exp} .

As mentioned previous, the most possible reason for the poorer correlation between $\langle W \rangle$ and ΔG_{exp} compared with the results by Ngo et al. maybe ascribe to the narrow range of activity. For the purpose of verifying the assumption, the ligand set was divided into two groups which can enlarge the span in activity of each group to some extent. The detailed grouping was shown in **Table S5, 6**.

Table S5. The six compounds of group 1 with the constructed mean work $\langle W \rangle$ for each conformation type.

Compound	ΔG_{exp} (Kcal/mol)	$\langle W \rangle$ (Kcal/mol)	
		Type A	Type B
1	-6.38	239.8 \pm 16.3	220.1 \pm 13.9
2	-7.79	189.7 \pm 10.2	232.7 \pm 13.2
3	-6.04	205.5 \pm 14.3	185.7 \pm 12.8
4	-5.93	162.8 \pm 7.6	200.0 \pm 15.4
5	-5.65	196.9 \pm 11.3	200.6 \pm 11.9
10	-5.49	182.7 \pm 16.2	182.9 \pm 12.6

Table S6. The six compounds of group 2 with the constructed mean work $\langle W \rangle$ for each conformation type.

Compound	ΔG_{exp} (Kcal/mol)	$\langle W \rangle$ (Kcal/mol)	
		Type A	Type B
2	-7.79	189.7 \pm 10.2	232.7 \pm 13.2
6	-6.31	194.5 \pm 16.2	208.2 \pm 14.9
7	-6.03	174.7 \pm 10.7	206.9 \pm 14.4
8	-5.70	176.8 \pm 12.9	197.9 \pm 14.1
9	-5.56	168.9 \pm 15.3	201.4 \pm 12.8
10	-5.49	182.7 \pm 16.2	182.9 \pm 12.6

According to the grouping mention above, the correlation between mean work $\langle W \rangle$ and experimental binding free energies ΔG_{exp} were constructed for the two types of binding modes, respectively (**Figure S3**). For conformation Type B, the obvious higher correlation ($R = -0.85, -0.93$) were observed for both groups. Meanwhile, $\langle W \rangle$ also exhibited stronger association with ΔG_{exp} ($R = -0.60$) for group 2 when compounds adopt

to conformation Type A, while group1 presented decreased correlation coefficient ($R = -0.13$) in comparison to the whole set ($R = -0.27$). The increased and strong correlation between $\langle W \rangle$ and ΔG_{exp} for both groups further proved that Type B was the most possible binding mode of the series of compounds.

Overall, this comparison indicated that the correlation between $\langle W \rangle$ and ΔG_{exp} becomes stronger with the expansion of activity scope, that is to say compounds with similar inhibitory activity can't be precisely and properly ranked by FPL method through constructing non-equilibrium work.

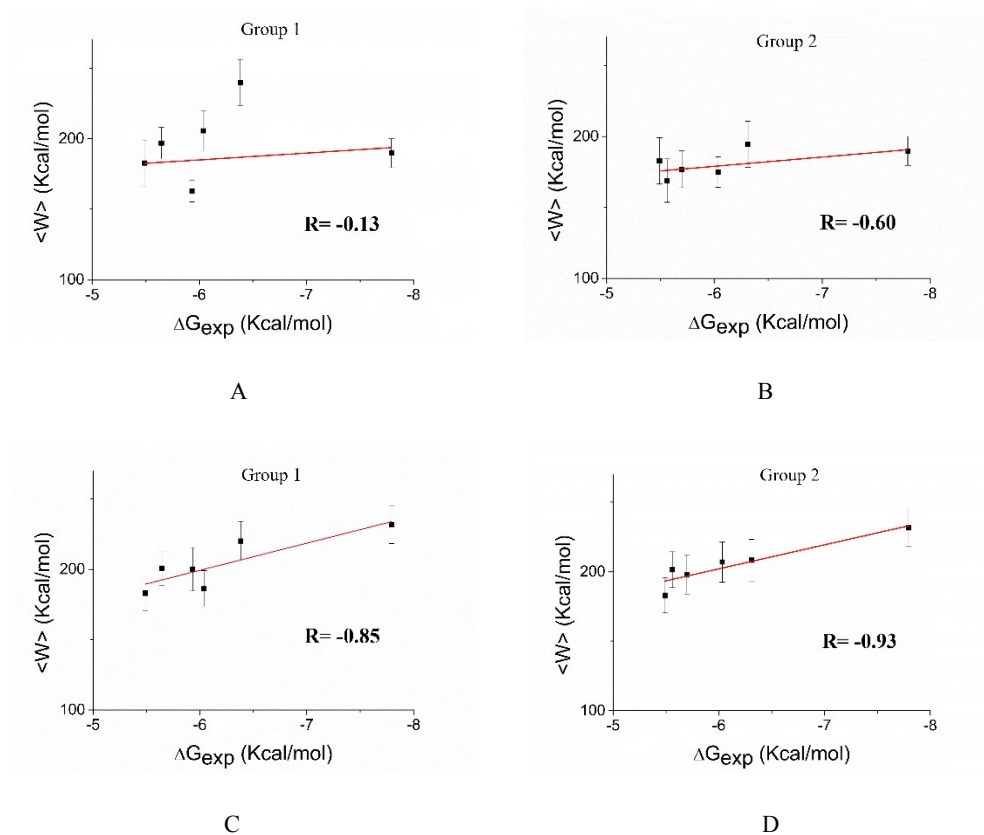


Figure S3. The correlation between $\langle W \rangle$ and ΔG_{exp} of conformation Type A for group 1 (A) and group 2(B). The correlation between $\langle W \rangle$ and ΔG_{exp} of conformation Type B for group 1 (C) and group 2(D)